Supplemental materials for

Effect of the Injection Structure on Gas Velocity Distribution in a 3D Vertical Oven

Qiucheng Zhou [1,], Zhanyu Yang [1], Changsong Zheng [1], Liping Wei [1,2,3,*], Dong Li [1,3,*], Xiaoyong Fan [4]

[1] *School of Chemical Engineering, Northwest University, Xi'an, Shaanxi 710069, China*

[2] *Xi'an Key Laboratory of Special Energy Materials, Northwest University, Xi'an, Shaanxi 710069, China*

[3] *The Research Center of Chemical Engineering Applying Technology for Resource of Shaanxi, , Xi'an, Shaanxi 710069, China*

[4] *School of Chemistry and Chemical Engineering, Shaanxi Key Laboratory of Low Metamorphic Coal Clean Utilization, Yulin University, Yulin 719000, Shaanxi, China*

***Corresponding author.**

Liping wei, weiliping@nwu.edu.cn

Contents

Simulation model

8 Figures

Simulation model

S.1 Conservation of mass for gas and solid phase

The gas mass balance equation is expressed as:

$$\frac{\partial}{\partial \mathrm{t}}\left(\rho_g \varepsilon_g\right) + \nabla \cdot \left(\rho_g \varepsilon_g \boldsymbol{u}_g\right) = 0 \tag{S1}$$

The mass balance equation of the solid phase is:

$$\frac{\partial}{\partial \mathrm{t}}\left(\rho_s \varepsilon_s\right) + \nabla \cdot \left(\rho_s \varepsilon_s \boldsymbol{u}_s\right) = 0 \tag{S2}$$

S.2 Momentum conservation equations

The momentum balance equation of gas phase is:

$$\frac{\partial}{\partial \mathrm{t}}\left(\varepsilon_g \rho_g \boldsymbol{u}_g\right) + \nabla \cdot \left(\varepsilon_g \rho_g \boldsymbol{u}_g \boldsymbol{u}_g\right) = -\varepsilon_g \nabla p + \nabla \cdot \tau_g + \varepsilon_g \rho_g \boldsymbol{g} - \beta\left(\boldsymbol{u}_g - \boldsymbol{u}_s\right) \tag{S3}$$

where, β is the gas–solid drag coefficient, τ_g is the gas viscous stress tensor.

$$\tau_g = \varepsilon_g \mu_g \left[\nabla \boldsymbol{u}_g + \nabla \boldsymbol{u}_g^T\right] - \frac{2}{3} \varepsilon_g \mu_g \nabla \cdot u_g \tag{S4}$$

The effective viscosity of gas phase μ_{g} includes two parts: dynamic viscosity μ_{gd} and turbulent viscosity μ_{gt}, which can be determined by solving the gas phase turbulence $k - \varepsilon$ models.

The momentum balance equation of mildly-cohesive solid phase is:

$$\frac{\partial}{\partial \mathrm{t}}\left(\varepsilon_s \rho_s \boldsymbol{u}_s\right) + \nabla \cdot \left(\varepsilon_s \rho_s \boldsymbol{u}_s \boldsymbol{u}_s\right) = -\varepsilon_s \nabla p + \nabla \cdot \tau_s - \nabla p_s + \varepsilon_s \rho_s \boldsymbol{g} + \beta\left(\boldsymbol{u}_g - \boldsymbol{u}_s\right) \tag{S5}$$

where, p_s is the solid pressure which represents the solids phase normal forces due to particle–particle interactions, τ_s is the solid viscous stress tensor.

$$\tau_s = \varepsilon_s \left\{\xi_s \nabla \boldsymbol{u}_s + \mu_s \left[\left(\nabla \boldsymbol{u}_s + \nabla \boldsymbol{u}_s^T\right) - \frac{2}{3} \nabla \cdot \boldsymbol{u}_s\right]\right\} \tag{S6}$$

where, ξ_s is the solid bulk viscosity which reflects the resistance of a fluid against

compression, μ_s is the solid shear viscosity which is in the same order of magnitude with bulk viscosity.

S.3 Typical kinetic model of granular flow

Solid pressure is expressed as below,

$$p_s = \rho_s \varepsilon_s \theta_s + 2 g_0 \rho_s \varepsilon_s^2 \theta_s (1+e) \tag{S7}$$

where, θ_s is the granular temperature $\theta_s = \frac{\boldsymbol{v}'^2}{3}$, $\boldsymbol{v}'$ is the fluctuating velocity, g_0 is the solid radial distribution function, e is the coefficient of restitution. The solid radial distribution function is:

$$g_0 = \left[1 - \left(\frac{\varepsilon_s}{\varepsilon_{s,max}}\right)^{\frac{1}{3}}\right]^{-1} \tag{S8}$$

The solid shear viscosity μ_s including the kinetic and collision terms is used:

$$\mu_s = \frac{5\rho_s d_p \sqrt{\pi\theta_s}}{48(1+e)g_0}\left[1 + \frac{4}{5} g_0 \varepsilon_s (1+e)\right]^2 + \frac{4}{5\sqrt{\pi}} \varepsilon_s \rho_s g_0 d_p \sqrt{\theta_s}(1+e) \tag{S9}$$

The bulk viscosity for a non-cohesive particle flow:

$$\xi_s = \frac{4}{3\sqrt{\pi}} \varepsilon_s \rho_s g_0 d_p (1+e)\sqrt{\theta_s} \tag{S10}$$

The conservation equation of fluctuating energy of particles can be expressed as:

$$\frac{3}{2}\left[\frac{\partial}{\partial \mathrm{t}}(\rho_s \varepsilon_s \theta_s) + \nabla \cdot (\rho_s \varepsilon_s \boldsymbol{u}_s \theta_s)\right] = (-\nabla p_s \boldsymbol{I} + \tau_s) : \nabla \boldsymbol{u}_s + \nabla \cdot (k_s \nabla \theta_s) - \gamma_s \tag{S11}$$

where, γ_s is the dissipation of fluctuating energy, k_s is the diffusion coefficient.

The dissipation of fluctuating energy is,

$$\gamma_s = 3(1-e^2)\varepsilon_s^2 \rho_s g_0 \theta \left(\frac{4}{d_s}\sqrt{\frac{\theta}{\pi}} - \nabla \cdot \boldsymbol{u}_s\right) \tag{S12}$$

The diffusion coefficient is expressed,

$$k_s = \frac{2}{\sqrt{\pi}} \varepsilon_s^2 \rho_s g_0 d_p (1+e)\sqrt{\theta_s} \tag{S13}$$

S.4 Drag force coefficients

The Gidaspow drag model is applied,

$$\varepsilon_{\mathrm{g}} \leq 0.8,\ \beta = 150\frac{{\varepsilon_{\mathrm{s}}}^2\mu_{\mathrm{g}}}{\varepsilon_{\mathrm{g}}d_{\mathrm{p}}^2} + 1.75\frac{\rho_{\mathrm{s}}|\boldsymbol{u}_{\mathrm{s}}-\boldsymbol{u}_{\mathrm{g}}|}{d_p} \tag{S14}$$

$$\varepsilon_{\mathrm{g}} > 0.8,\ \beta = \frac{3}{4}C_D\frac{\varepsilon_{\mathrm{s}}\varepsilon_{\mathrm{g}}\rho_{\mathrm{s}}|\boldsymbol{u}_{\mathrm{s}}-\boldsymbol{u}_{\mathrm{g}}|}{d_p}\varepsilon_g^{-2.65} \tag{S15}$$

$$C_D = \begin{cases} \frac{24}{\varepsilon_g Re_{\mathrm{s}}}\left[1 + 0.15\left(\varepsilon_{\mathrm{g}}Re_{\mathrm{s}}\right)^{0.687}\right], Re_{\mathrm{s}} \leq 1000 \\ 0.44, Re_{\mathrm{s}} \geq 1000 \end{cases} \tag{S16}$$

$$Re_{\mathrm{s}} = \frac{\varepsilon_{\mathrm{s}}\rho_{\mathrm{g}}d_p|\boldsymbol{u}_{\mathrm{s}}-\boldsymbol{u}_{\mathrm{g}}|}{\mu_g} \tag{S17}$$

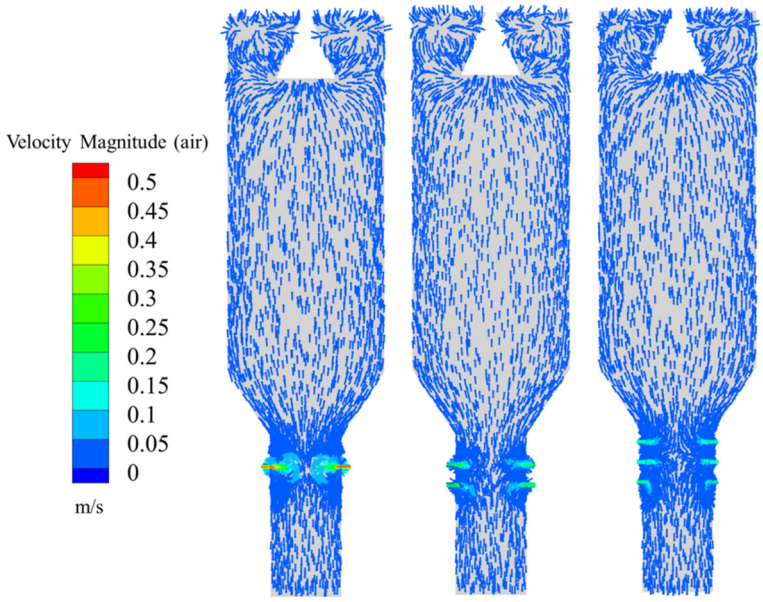

(a) Gas velocity vectors through in-central cross-section

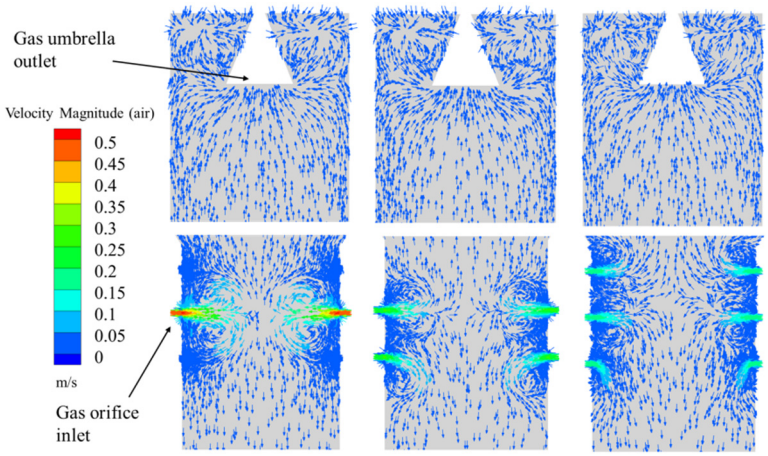

(b) Gas velocity distribution near the gas orifice inlet and umbrella outlet

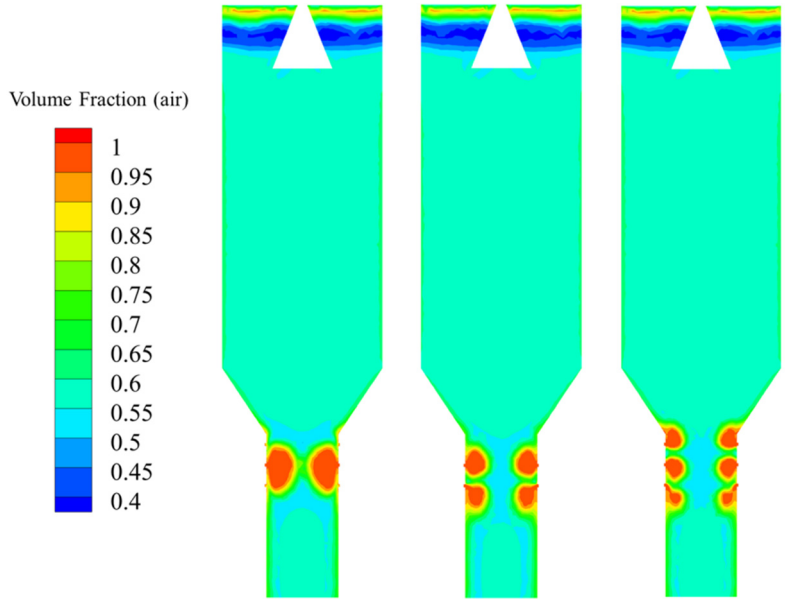

(c) Air fraction distribution

Figure S1: Effect of layers of gas orifice on gas distribution, (a) Gas velocity vectors through in-central cross-section, (b) Gas velocity distribution near the gas orifice inlet and umbrella outlet, (c) Air fraction distribution (t=20s), d_p= 6 mm, u_g=0.24 m/s and u_S=4.2× 10^4 m/s

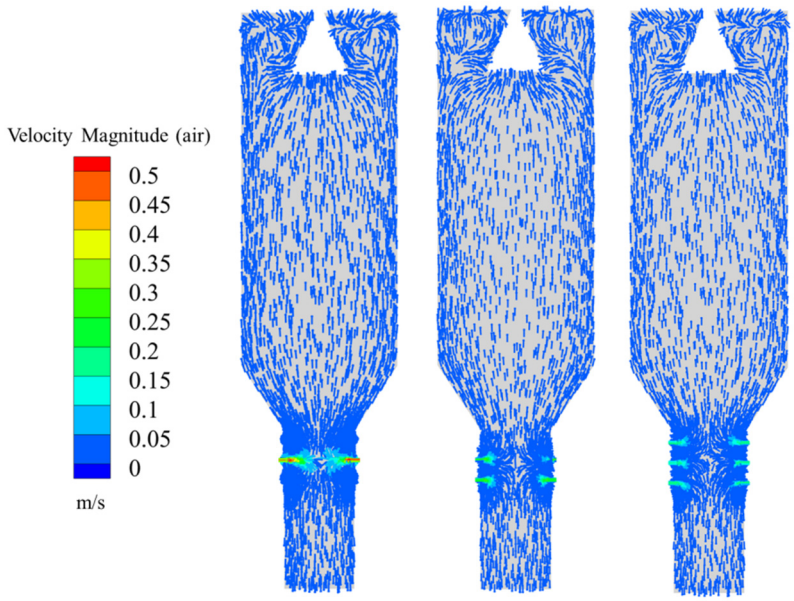

(a) Gas velocity vectors through in-central cross-section

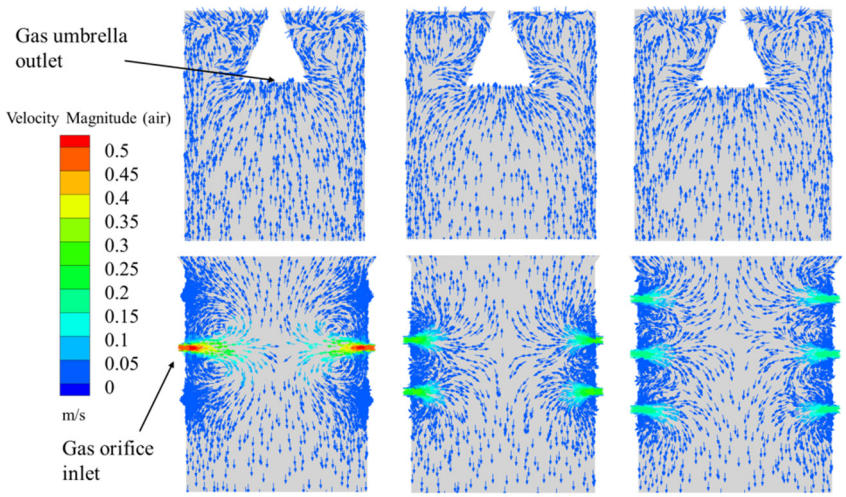

(b) Gas velocity distribution near the gas orifice inlet and umbrella outlet

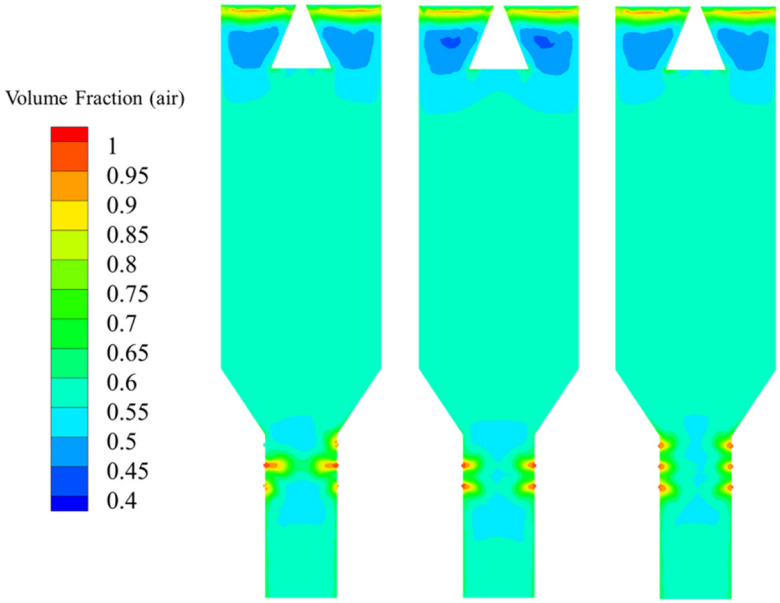

(c) Air fraction distribution

Figure S2: Effect of layers of gas orifice on gas distribution,(a) Gas velocity vectors through in-central cross-section, (b)Gas velocity distribution near the gas orifice inlet and umbrella outlet, (c) Air fraction distribution (t=20s), d_p= 30 mm, u_g=0.24 m/s and u_S=4.2× 10^4 m/s

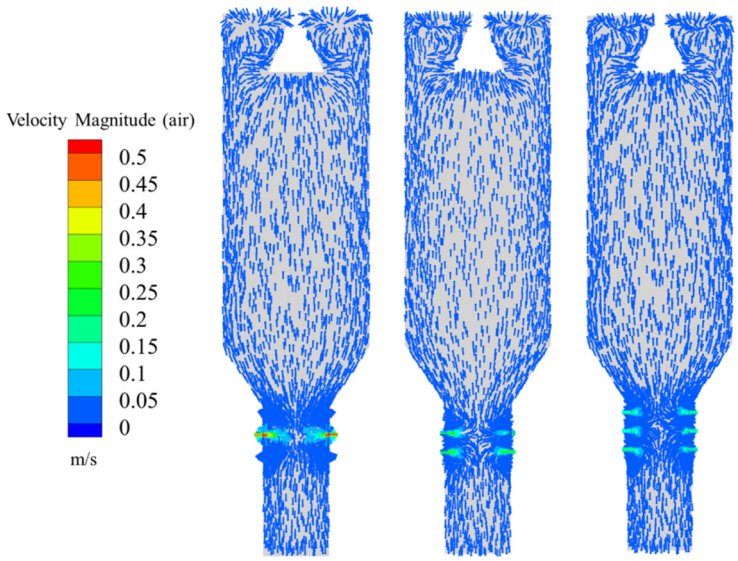

(a) Gas velocity vectors through in-central cross-section

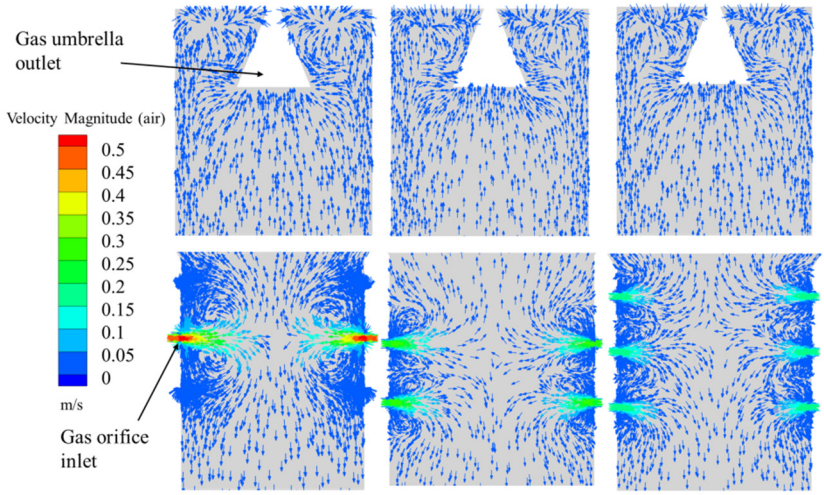

(b) Gas velocity distribution near the gas orifice inlet and umbrella outlet

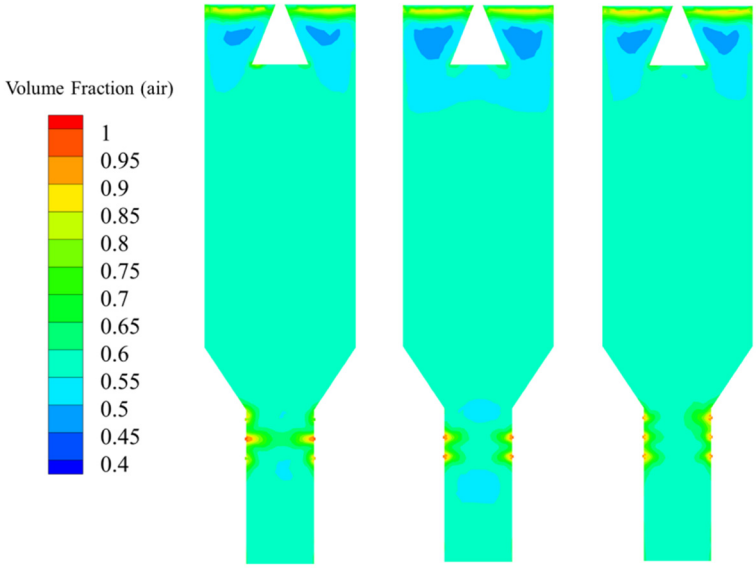

(c) Air fraction distribution

Figure S3: Effect of layers of gas orifice on gas distribution, (a) Gas velocity vectors through in-central cross-section, (b) Gas velocity distribution near the gas orifice inlet and umbrella outlet, (c) Air fraction distribution (t=20s), d_p= 50 mm, u_g=0.24 m/s and u_S=4.2× 10^4 m/s

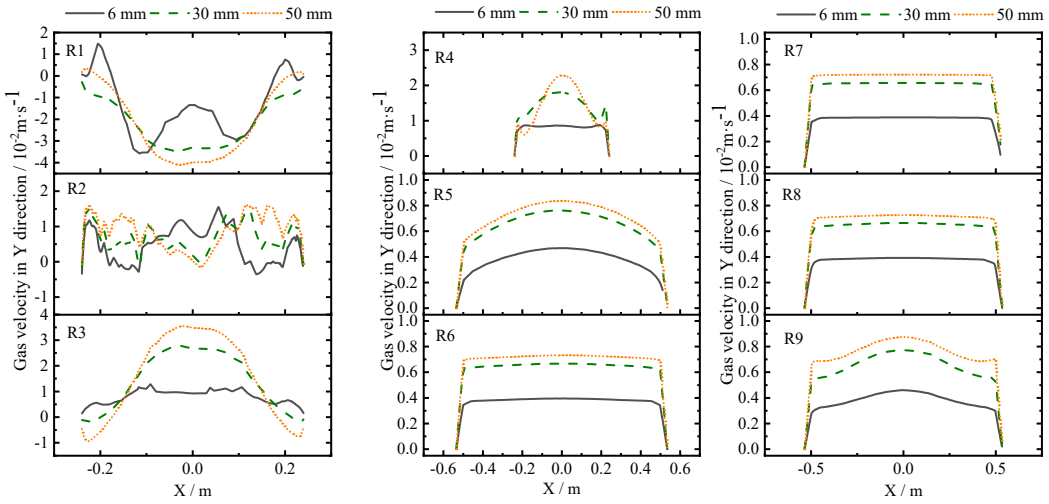

(a) One layer

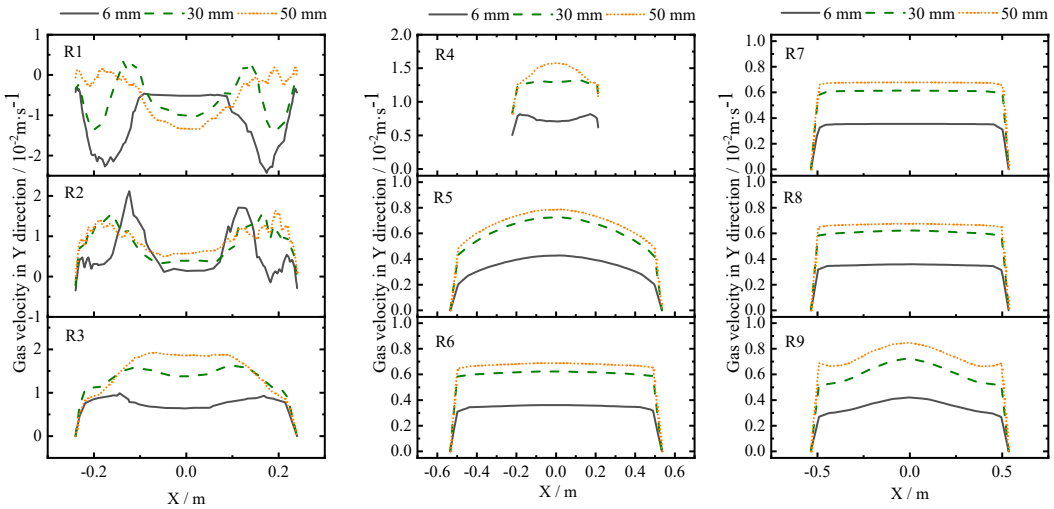

(b) Two layers

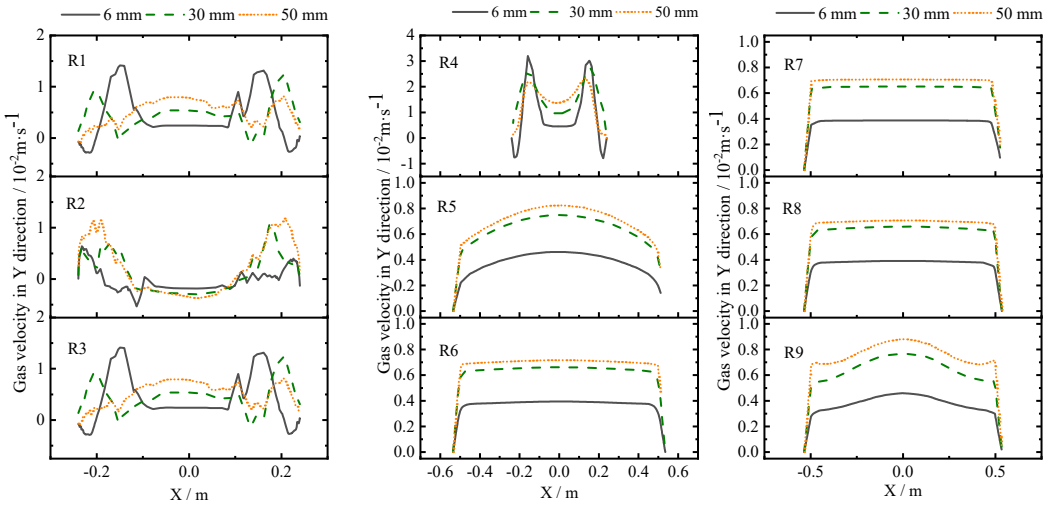

(c) Three layers

Figure S4: Variation of gas velocity in Y direction with increasing bed height under the effect of layers of orifice, (a) one layer, (b) two layers, (c) three layers

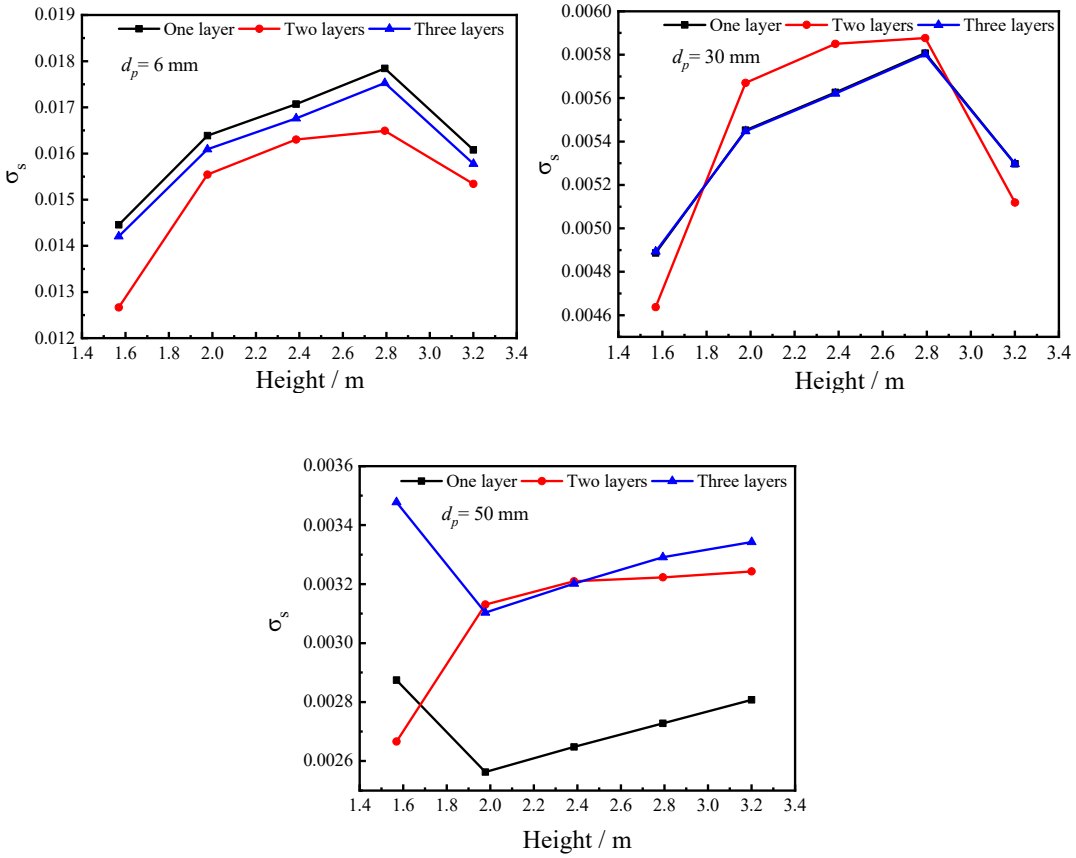

(a) Coal solid fraction standard deviation

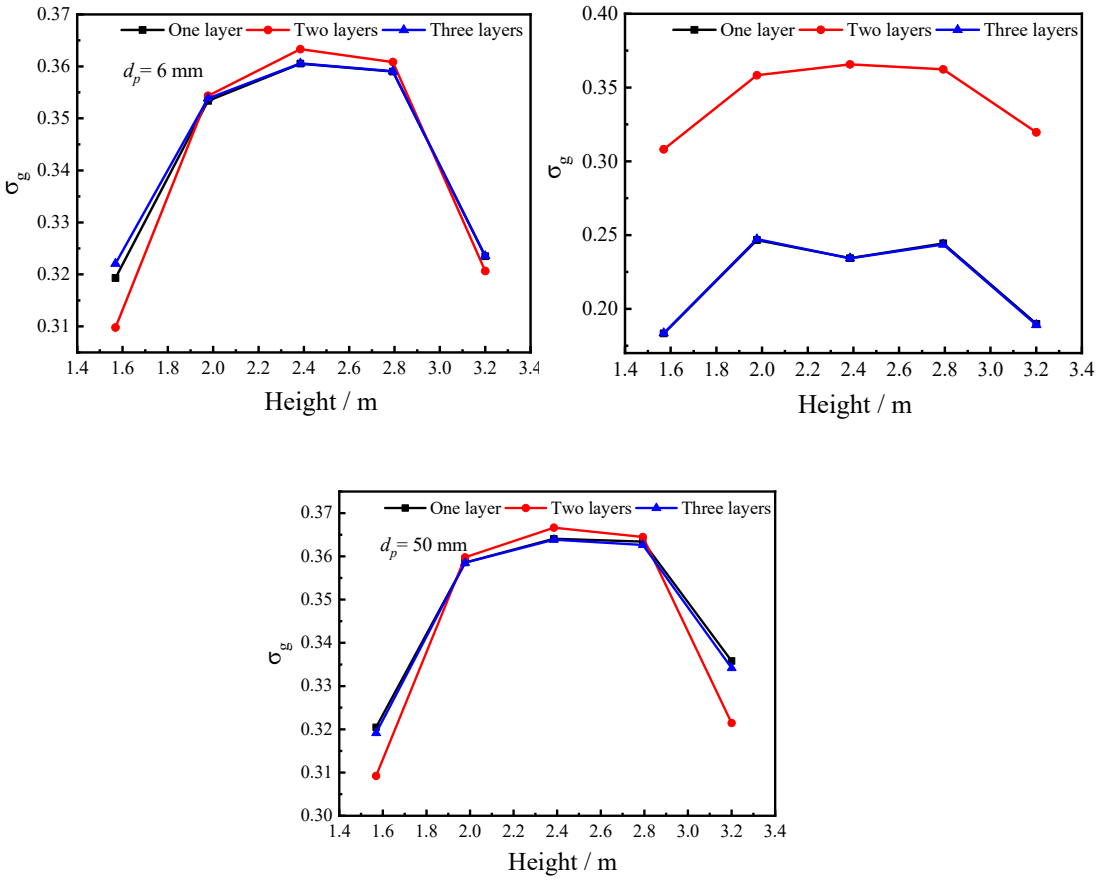

(b) gas velocity standard deviation

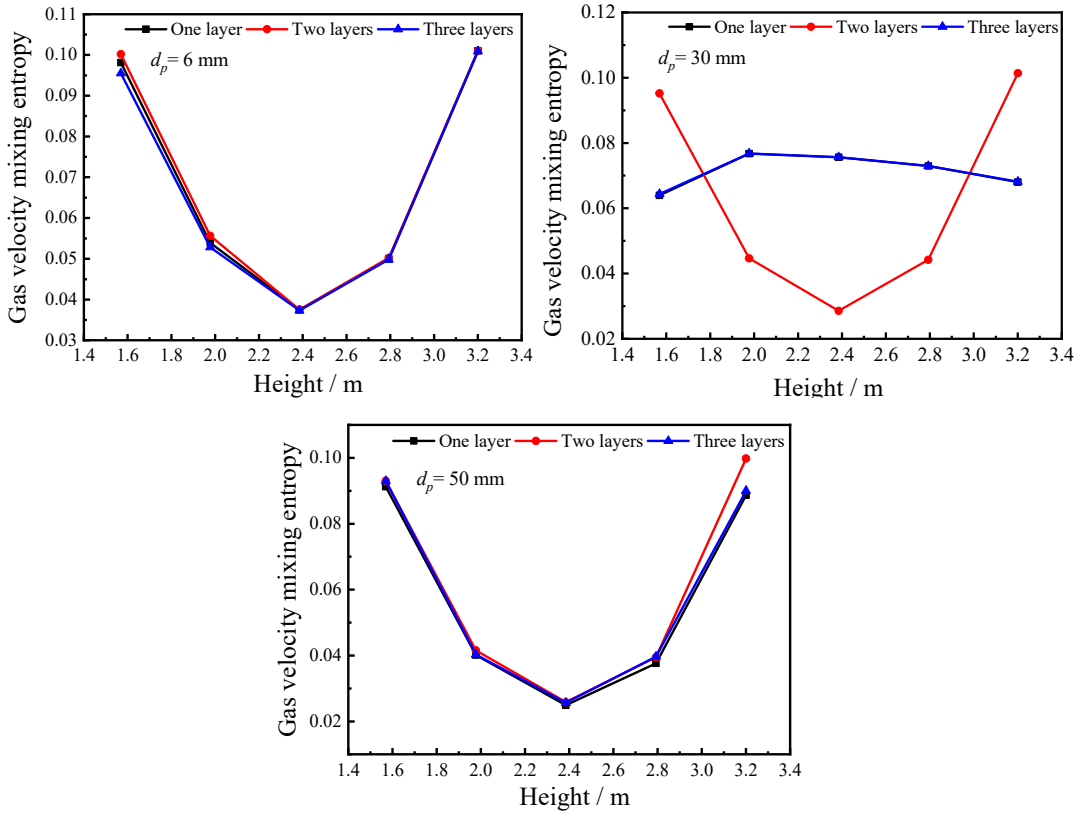

(c) gas velocity mixing entropy

Figure S5: Influence of gas injection layers on gas distribution in the pyrolysis zone, (a) Coal solid fraction standard deviation, (b) Gas velocity standard deviation, (c) Gas velocity mixing entropy, u_g=0.24 m/s and u_s=4.2× 10^{-4} m/s

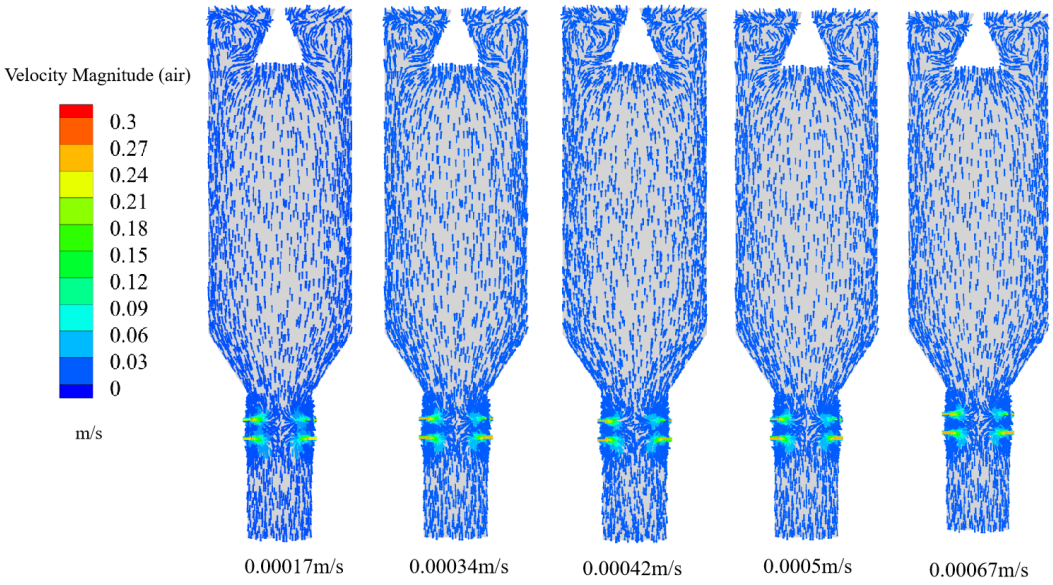

(a) Gas velocity vectors through in-central cross-section

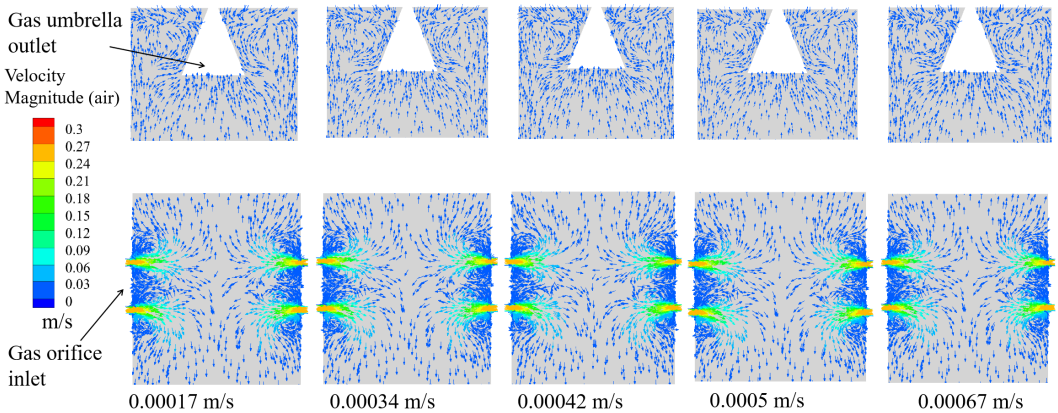

(b) Gas velocity distribution near the gas orifice inlet and umbrella outlet

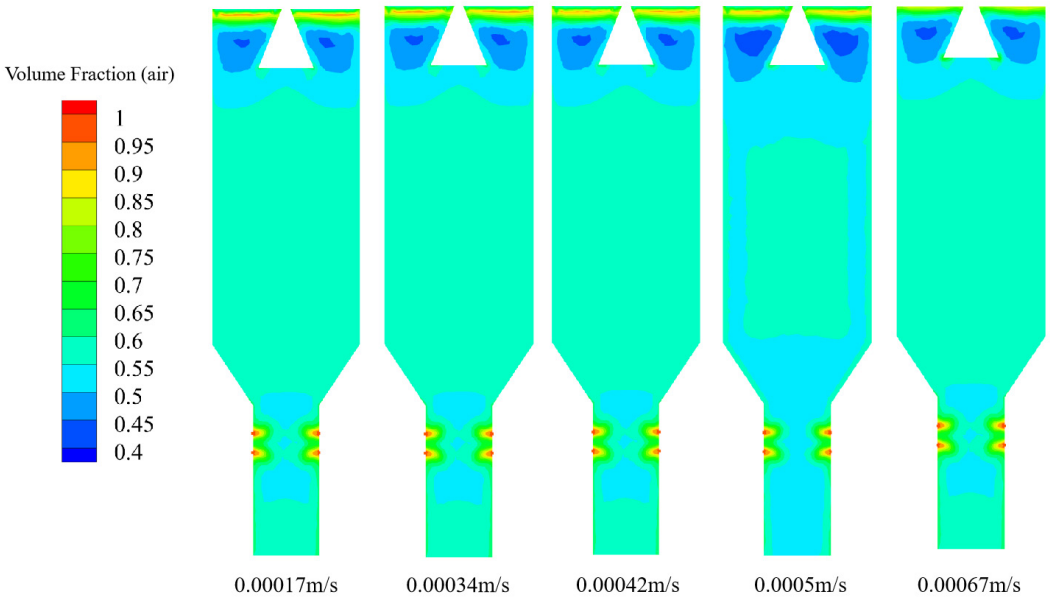

(c) Air fraction distribution

Figure S6 Influence of coal feeding rate on gas distribution, (a) Gas velocity vectors through in-central cross-section, (b)Gas velocity distribution near the gas orifice inlet and umbrella outlet, (c) Air fraction distribution （t = 20s） d_P **= 30 mm,** u_g **= 0.24 m/s**

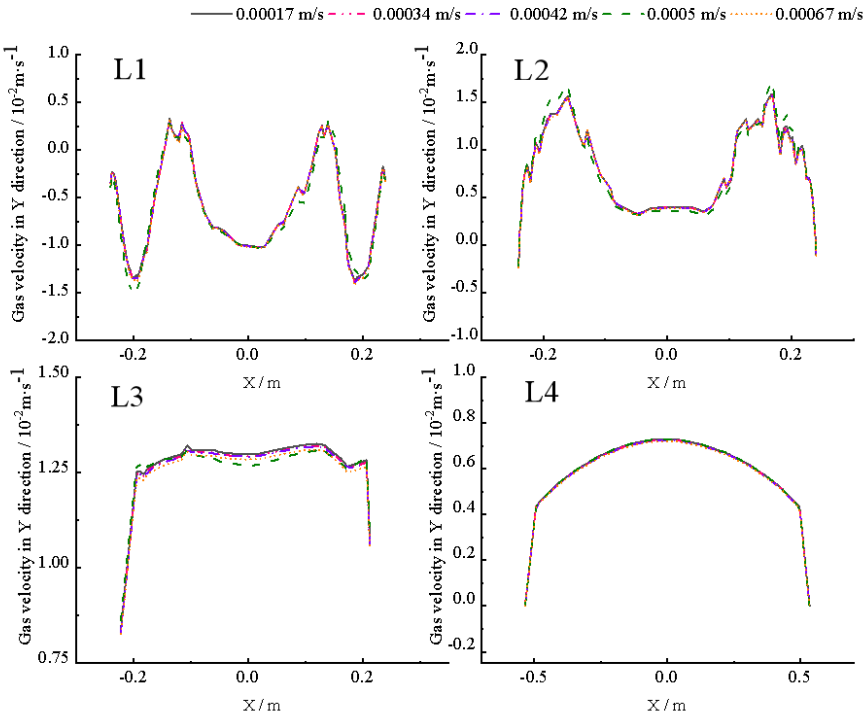

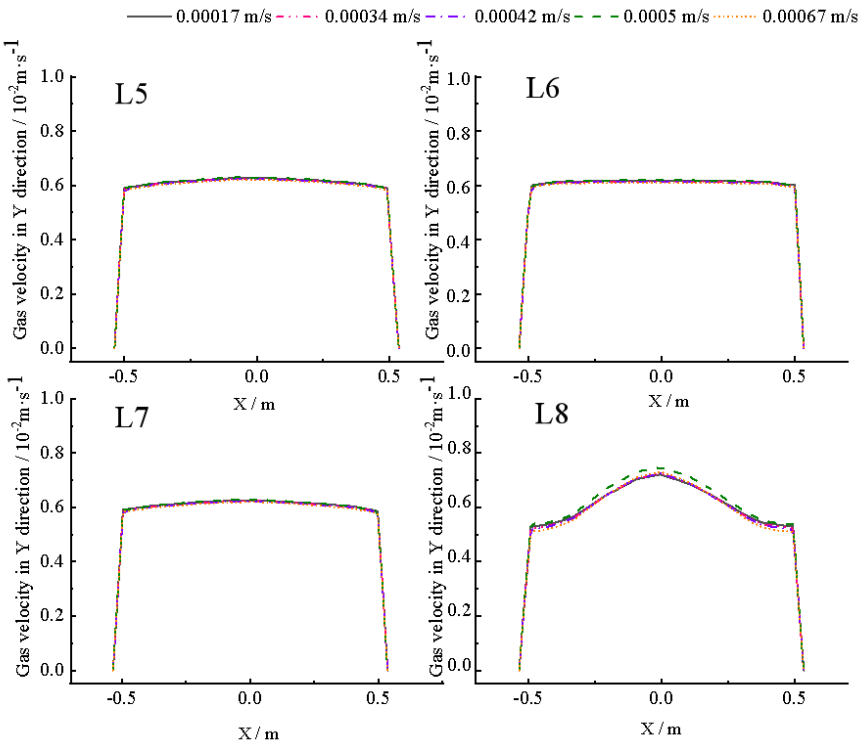

Figure S7 Variation of gas velocity in Y direction with increasing bed height under the effect of coal feeding rate.

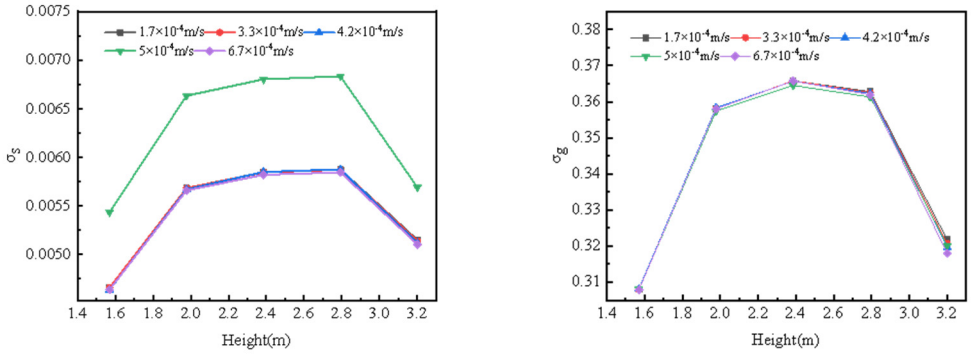

(a) Coal solid fraction standard deviation *(b) Gas velocity standard deviation*

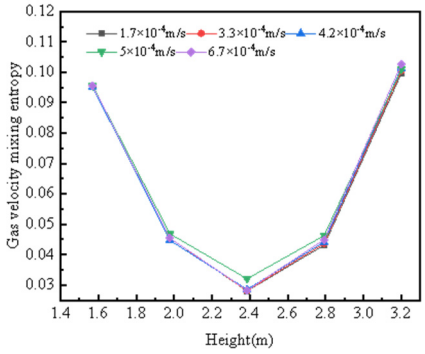

(c) Gas velocity mixing entropy

Figure S8 Influence of coal feeding rate on gas distribution in the pyrolysis zone (a) Coal solid fraction standard deviation, (b) Gas velocity standard deviation, (c) Gas velocity mixing entropy, $\boldsymbol{d_P}$ **= 30 mm,** $\boldsymbol{u_g}$ **= 0.24 m/s**